Electronic Supplementary Information

Deciphering amplification of dual catalytic active sites of Se-doped NiV LDH in water electrolysis: A hidden gem exposure of anion doping at core-lattice LDH framework

Aditi De, [†‡] ***Ragunath Madhu,*** [†‡] ***Krishnendu Bera,*** [†‡] ***Hariharan N Dhandapani,*** [†‡] ***Sreenivasan Nagappan,*** [†‡] ***Suprobhat Singha Roy,*** [†‡] ***and Subrata Kundu*** [†‡]*

[†]*Academy of Scientific and Innovative Research (AcSIR), Ghaziabad-201002, India.*

[‡]*Electrochemical Process Engineering (EPE) Division, CSIR-Central Electrochemical Research Institute (CECRI), Karaikudi-630003, Tamil Nadu, India.*

*To whom correspondence should be addressed, *E-mail:* skundu@cecri.res.in; kundu.subrata@gmail.com. Phone/Fax: (+ 91) 4565-241487.

This file contains 29 pages in which the specification of reagents, methods of synthesis, instruments used in the study, electrochemical characterization, electrochemical results, characterizations like XRD, HR-TEM images, EDS, XPS, post-FESEM, post-HR-TEM images, post-XPS, comparison table, references are given.

No. of Figure: 18

No. Table: 3

Figures	The subject of the Figure	Page number
S1	XRD spectrum of the Se-NiV LDH and NiV LDH over Ni foam	**S7**
S2	HR-TEM images of NiV LDH with lattice fringes pattern and SAED pattern	**S8**
S3	HAADF colour mapping analysis and colour mapping result of the mix, Ni K shell, V K shell, O K shell, and C K shell	**S9**
S4	EDS spectrum of NiV LDH and Se-NiV LDH at HR-TEM mode	**S10**
S5	The deconvoluted XPS Survey spectra of; (a) NiV LDH; and (b) Se-NiV LDH	**S11**
S6	The deconvoluted XPS spectrum of Se 3d orbitals of Se-NiV LDH.	**S12**
S7	Bar diagram of OER overpotential values comparison for NiV LDH and Se-NiV LDH catalysts	**S13**
S8	The area of the reduction peaks of; (a) Se-NiV LDH and (b) NiV LDH catalyst	**S14**
S9	CVs recorded for (a) NiV LDH; and (b) Se-NiV LDH in a non-faradic region with increasing scan rate for the determination of ECSA from the double layer capacitance	**S15**
S10	ECSA normalized polarization curve of NiV LDH and Se-NiV LDH	**S16**
S11	(a) OER polarisation curve for NiV LDH and Se-NiV LDH before and after AD (b) Corresponding EIS values	**S17**
S12	(a) HER polarisation curve for NiV LDH and Se-NiV LDH before and after AD (b) Corresponding EIS values	**S18**
S13	Predicted Band structures and Fermi energy level comparison for NiV LDH and Se-NiV LDH	**S19**
S14	(a-c) Low to high magnified FE-SEM images of post-Se-NiV LDH. (d) EDS spectrum of post-Se-NiV LDH	**S20**
S15	(a) High-magnified post-HRTEM images of post-Se-NiV LDH. (b) SAED pattern of post-Se-NiV LDH. (c) HAADF image of post-Se-NiV LDH taken for mapping analysis, (d-i) are the characteristic colour mapping results of mix, Ni, V, Se, O, and C, respectively	**S21**
S16	The deconvoluted post-XPS (a) Survey spectra; (b) Ni 2p orbitals; (c) V 2p+O 1s orbitals and (d) Se 3d orbitals of Se-NiV LDH	**S22**
S17	The deconvoluted post-XPS spectrum of Se 3p orbitals of Se-NiV LDH	**S23**
S18	The post-FESEM, HRTEM images of of Se-NiV LDH	**S24**
Table S1	Comparison table for OER activity of Se-NiV LDH with a similar type of catalyst	**S25**
Table S2	Comparison table for HER activity of Se-NiV LDH with a similar type of catalyst	**S26**
Table S3	Comparison table for TWS activity of Se-NiV LDH with a similar type of catalyst	**S27**
	References	**S28-S29**

Reagents and Instruments:

Nickel Nitrate [$Ni(NO_3)_2.6H_2O$], Vanadium Chloride [VCl_3], Urea $CO(NH_2)_2$, Se powder, ammonium fluoride [NH_4F], DMF, Hydrazine [N_2H_4] were purchased from Sigma-Aldrich and used as received. Sodium carbonate (Na_2CO_3) was purchased from Merck and used as received. Ni foam was procured from Sigma-Aldrich and used after surface cleaning. The electrochemical analyzer AURT-M204 was used for all electrochemical characterizations. Hg/HgO reference electrode (in 1 M KOH) purchased from CH instruments and platinum (Pt) (for OER), and graphite rod (for HER) as counter electrodes from Alfa-Aesar were used throughout the electrochemical studies along with the Ni foam with materials grown as working electrodes. DI water was used throughout the entire experiment. The as-prepared catalysts with different stoichiometric ratios were characterized with HR-TEM, (TecnaiTM G2 TF20) working at an accelerating voltage of 200 kV and by Talos F-200-S with HAADF elemental mapping. Color mapping and Energy Dispersive X-ray Spectroscopy (EDS) analysis were carried out with the FESEM instrument with the images (SUPRA 55VP Carl zeiss) with a separate EDS detector connected to that instrument. The XRD analysis carried out with a scanning rate of 5° min-1 in the 2θ range 10-90° using a Rigaku X-ray powder diffractometer (XRD) with Cu Kα radiation ($\lambda = 0.154$ nm). X-ray photoelectron spectroscopic (XPS) analysis was performed using a Theta Probe AR-XPS system (Thermo Fisher Scientific, UK). The Bruker Tensor 27 (Optik GmbH, Germany) with an RT DLaTGS (Varian) detector was used for FT-IR analysis. LASER Raman spectroscopic measurements were carried out by green emitting semiconductor as a laser source of 532 nm. For Raman experiment the excitation light intensity is about approximately 10 mW with a spectral collection of time of 1 sec. The integration time for our measurement was set to be 10 s.

Electrochemical Characterizations:

The electrochemical workstation AURT-M204 had been used for the entire total water splitting studies. Electrocatalytic studies were done with the conventional three-electrode system. For the OER experiment, we used Pt as a counter electrode and for HER graphite rod is used as counter electrode. The Hg/HgO electrode has been used as a reference electrode for OER and HER, the working electrode is the synthesized catalysts over Ni foam. The polarization studies were carried out at a slow scan rate of 5 mV/sec. 50% iR compensation was done manually from the Rs from EIS. Continuous rapid sweeping through accelerated degradation (AD) studies at a very high sweep rate of 200 ms^{-1} for 500 cycles were Carried out in 1 M KOH for OER and also for HER. For handling the chemicals and glassware for the synthesis process as well as the application part, safety gloves, lab coats, and safety glass were mandatory and used accordingly.

All the resulting potential data that were collected by taking Hg/HgO as a reference electrode were later converted with respect to the reversal hydrogen electrode (E_{RHE}) by considering the Nernst equation of

$$E_{RHE} = E_{ref} + 0.059 \times 14 + 0.098 \quad \text{……Equation S1}$$

Over potential (η) values of all the catalysts at benchmarking current density of 10 mA/cm^2 calculation has been done by following this equation

$$\eta = E_{RHE} - 1.23\ V \quad \text{……Equation S2}$$

Tafel slope was calculated by fitting η *vs* log(j) using the Tafel equation

$$\eta = b \cdot \log(j/j_0) \quad \text{……Equation S3}$$

where b represents the Tafel slope, j signifies the current density and j_0 is the exchange current density. Electrochemical impedance spectroscopy (EIS) measurements were done on the frequency ranges from 10^5 to 1 Hz at 300 mV *vs* RHE. The value of electrochemical active

surface areas (ECSA) can be measured by determining the electrochemical double layer capacitance (C_{dl}) as follows:

$$i_c = \nu \times C_{dl} \ldots\ldots\ldots\ldots \text{Equation S4}$$

$$\text{ECSA} = \frac{C_{dl}}{C_s} \ldots\ldots\ldots \text{Equation S5}$$

Where i_c indicates the double-layer charging current resulting from scan-rates (ν) dependent CVs at non-faradic potential, C_s denotes a specific capacitance value of 0.040 mF/cm^2 depending on the typical reported values.

All the electrodes have been fabricated by the conventional drop-casting method for 20 cycling in a slow scan rate in order to understand activity by means of decreasing onset potential value after Se doping. Typically, the catalyst ink was prepared by taking 3 mg of catalyst powder in a solution mixture containing 750 µl of H_2O, 200 µl of ethanol, and 50 µl of 5% Nafion solution. Then 34.5 ml of catalyst ink was drop-casted over carbon with an effective surface area of 1×0.5 cm^2.

$$\text{Hence, loading is} = \frac{3 \times 34.5}{1000} \sim 0.1045 \text{ mg of catalyst} \ldots\ldots\ldots \text{Equation S6}$$

❖ **Determination of Surface concentration of various materials from the redox features of CV:**

- Calculated area associated with the reduction of Ni^{3+} to Ni^{2+} of **NiV LDH** = 0.003125VA

Hence, the associated charge is = 0.003125VA / 0.005 Vs^{-1}

= 0.625 As

= 0.625 C

Now, the number of electrons transferred is = 0.625 C / 1.602 ×10^{-19}

$$= \mathbf{3.9013\times10^{18}}$$

Since the reduction of Ni^{3+} to Ni^{2+} is a single electron transfer reaction, the number of electrons calculated above is exactly the same as the number of surface-active sites.

Hence, the number of Ni participating in OER is = **3.9013×10^{18}**

In our study, the determination of Turnover Frequency (TOF) from OER Current Density TOF was calculated assuming that the surface-active Ni atoms that had undergone the redox reaction just before the onset of OER only participated in OER electrocatalysis. The corresponding expression is,

$$TOF = j \times N_A / F \times n \times \Gamma$$

Where, j = current density, N_A = Avogadro number, F = Faraday constant, n = Number of electrons, Γ = Surface concentration.

Hence, for NiV LDH at 1.55V, we have the TOF value of

$$TOF_{1.55\ V} = [(46\times10^{-3})\ (6.023\times 10^{23})] / [(96485)\ (4)\ (3.9013\times10^{18})]$$

$$= \mathbf{0.0184\ sec^{-1}}$$

- Similarly, we calculated the TOF value for the Se-NiV LDH and $TOF_{1.55\ V}$ = **0.0359 sec^{-1}**
- In the case of HER reaction TOF was calculated by considering the area of the C_{dl} curve to calculate surface concentration value and the obtained TOF values at -0.213V for **NiV LDH** and **Se-NiV LDH for HER 0.246** and **0.4618 s^{-1}** respectively.

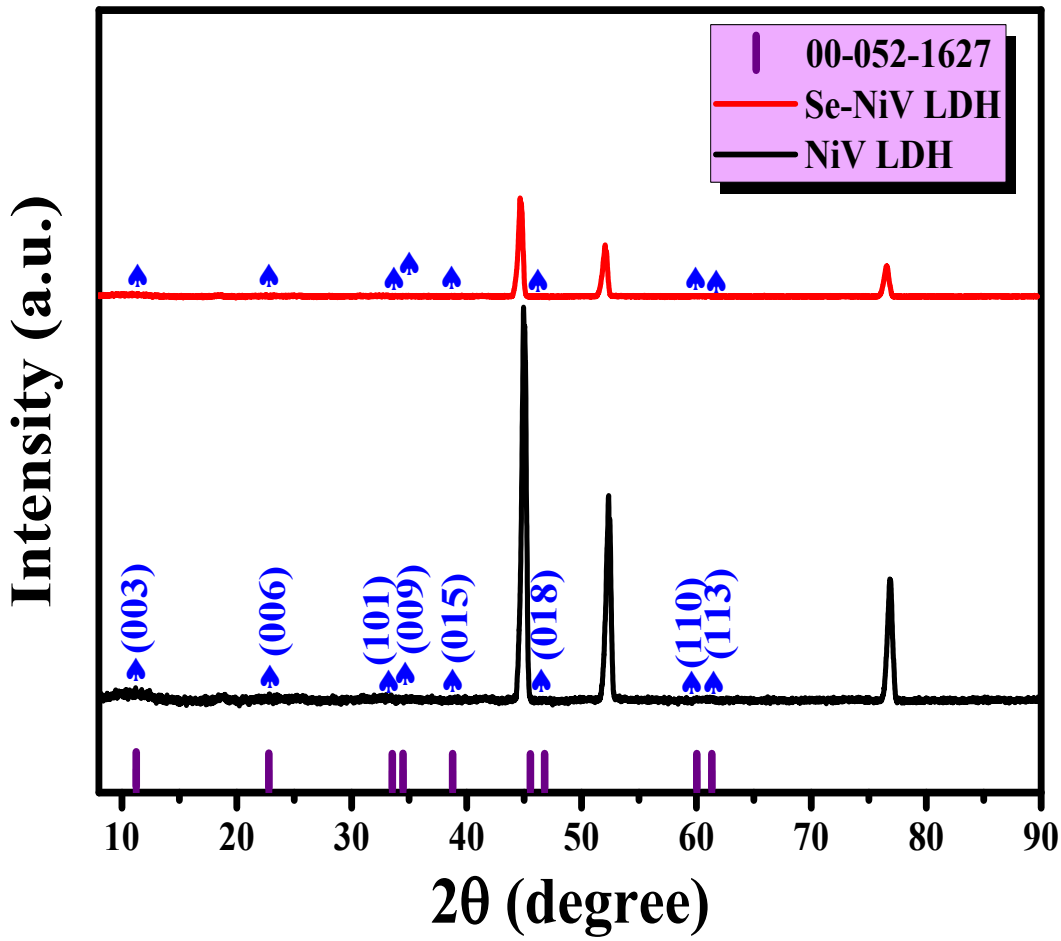

Figure S1: *(a) XRD pattern of Se-NiV LDH and NiV LDH over Ni foam from top to bottom respectively.*

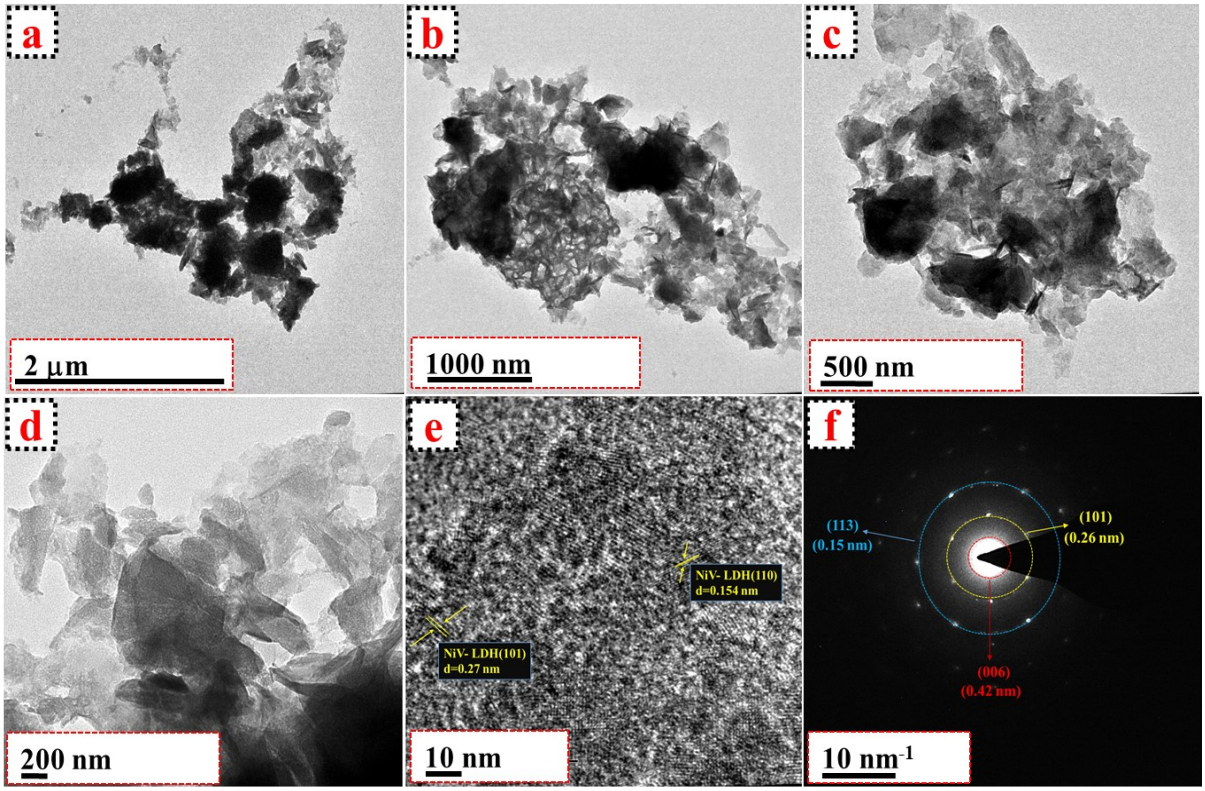

Figure S2: *(a-d) Low to high HR-TEM magnified images of NiV LDH. (e) Lattice fringes pattern of NiV LDH. (f) SAED pattern of NiV LDH.*

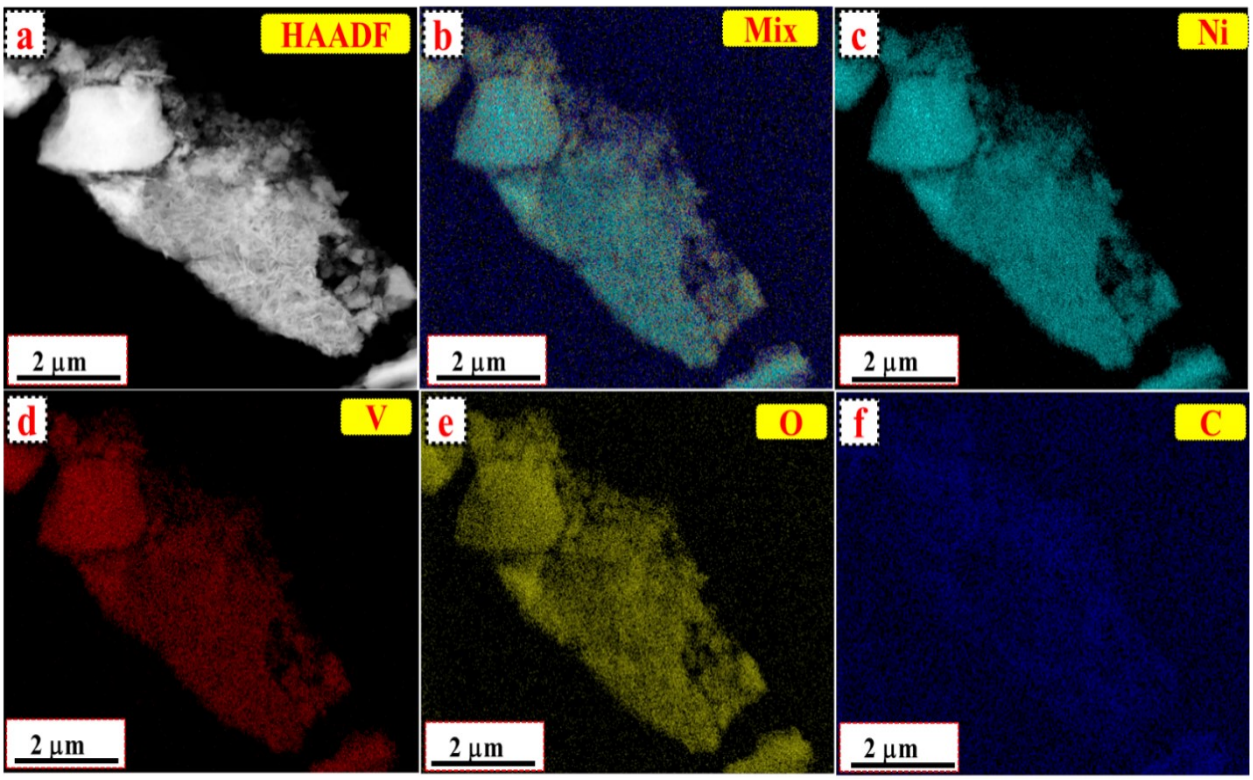

Figure S3: *(a) HAADF image of NiV LDH taken for mapping analysis, (b-f) are the characteristic colour mapping results of mix, Ni, V, O, and C of NiV LDH respectively.*

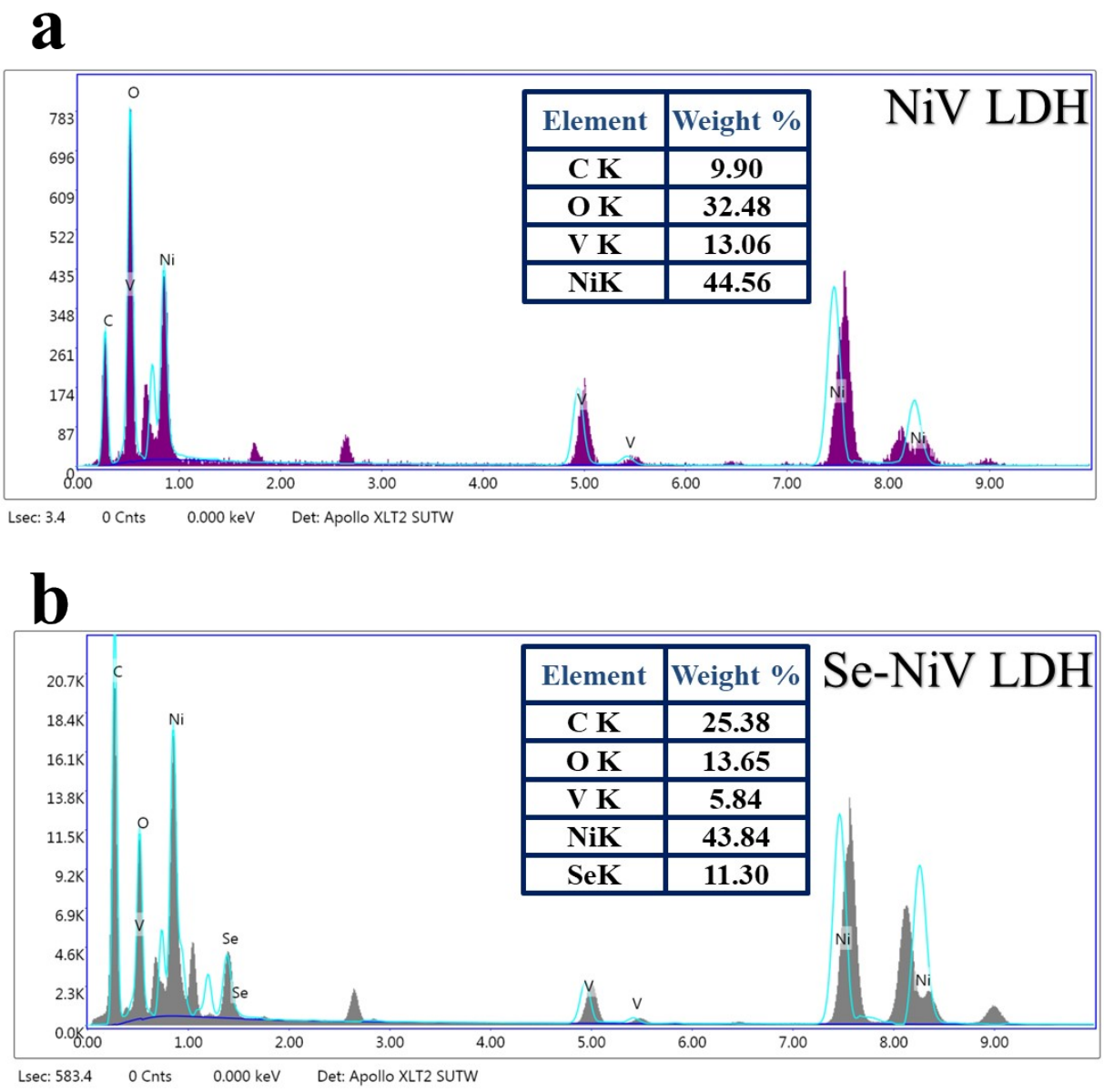

Figure S4: *(a) EDS spectrum of NiV LDH and Se-NiV LDH at HR-TEM mode.*

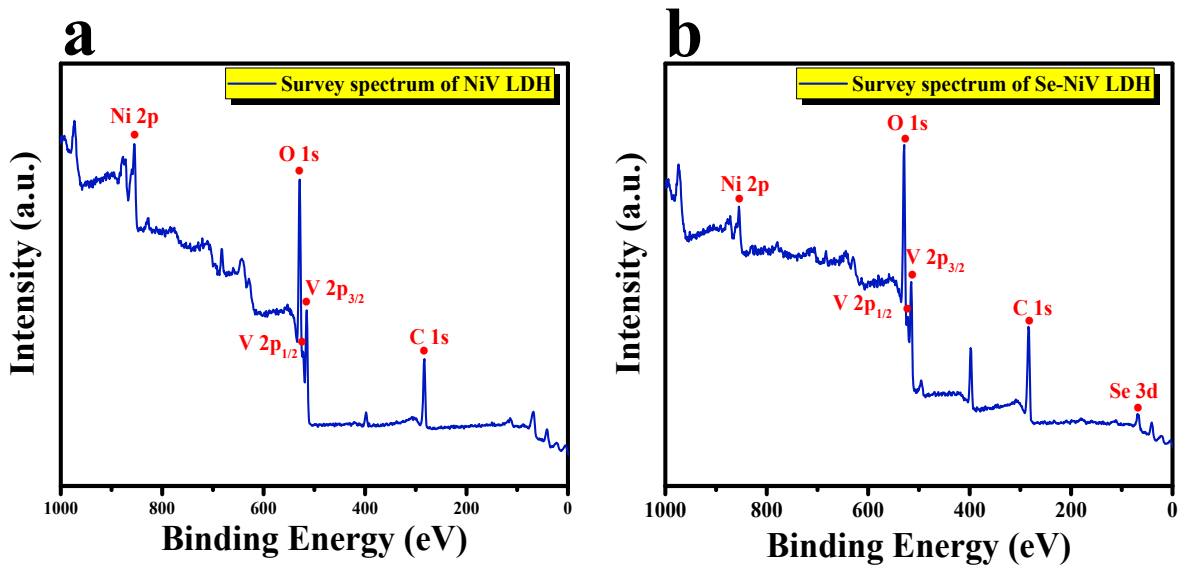

Figure S5: *XPS survey spectrum of (a) NiV LDH; and (b) Se-NiV LDH.*

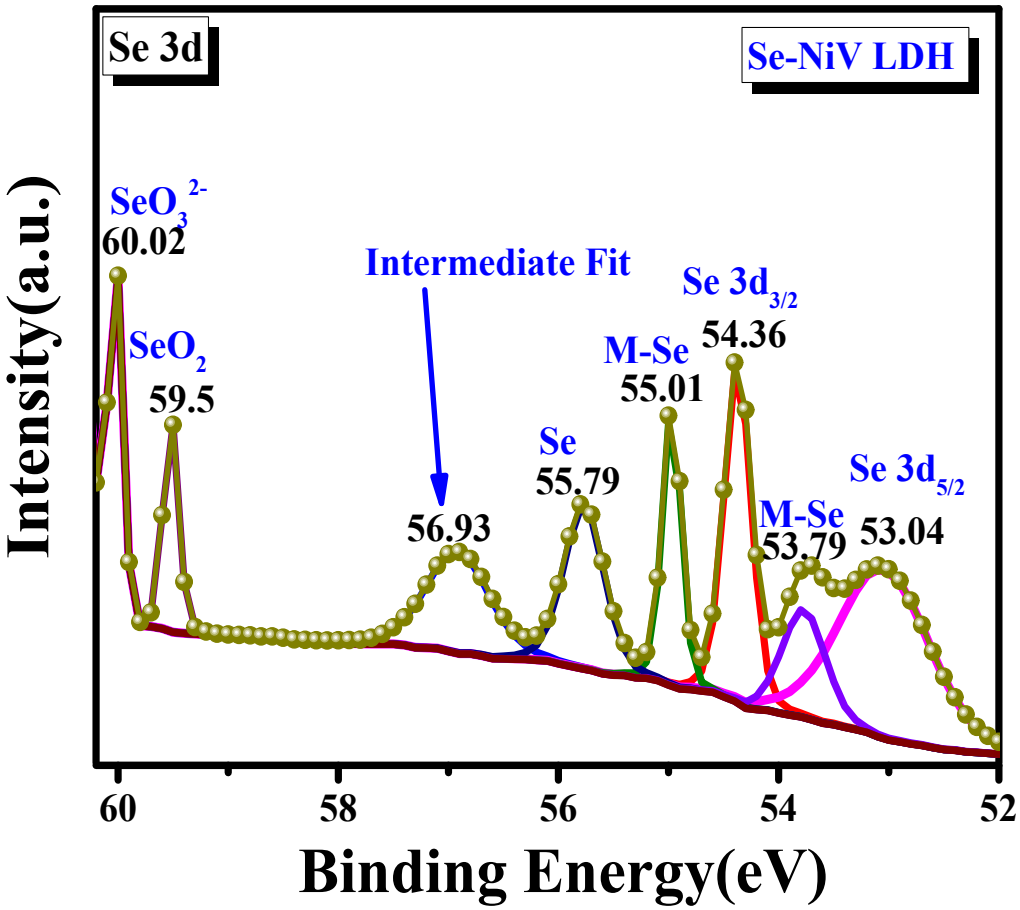

Figure S6: *(a) Deconvoluted XPS spectrum of Se 3d orbitals of Se-NiV LDH.*

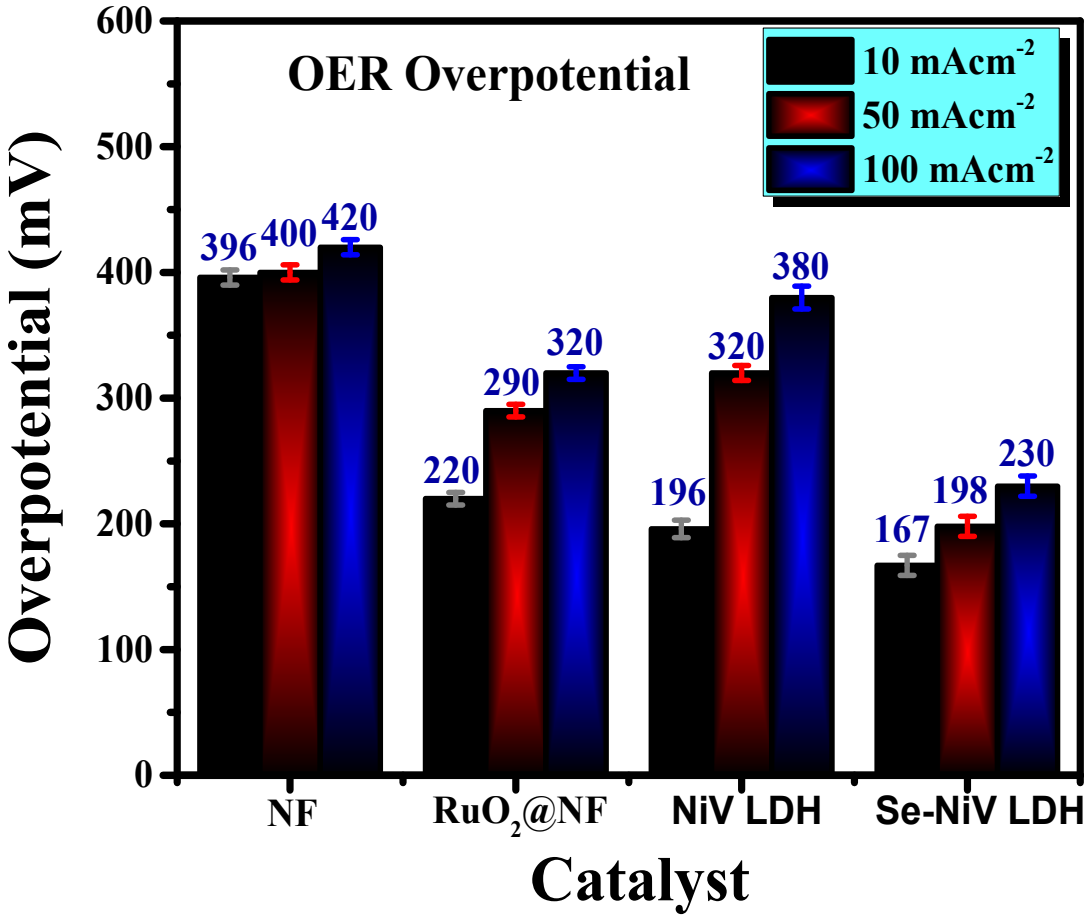

Figure S7: *Bar diagram of OER overpotential values measured at different current density values (10, 50, 100 mA cm^{-2}) for NiV LDH and Se-NiV LDH catalysts comparing with the state-of-art RuO2 catalyst with the same catalyst loading.*

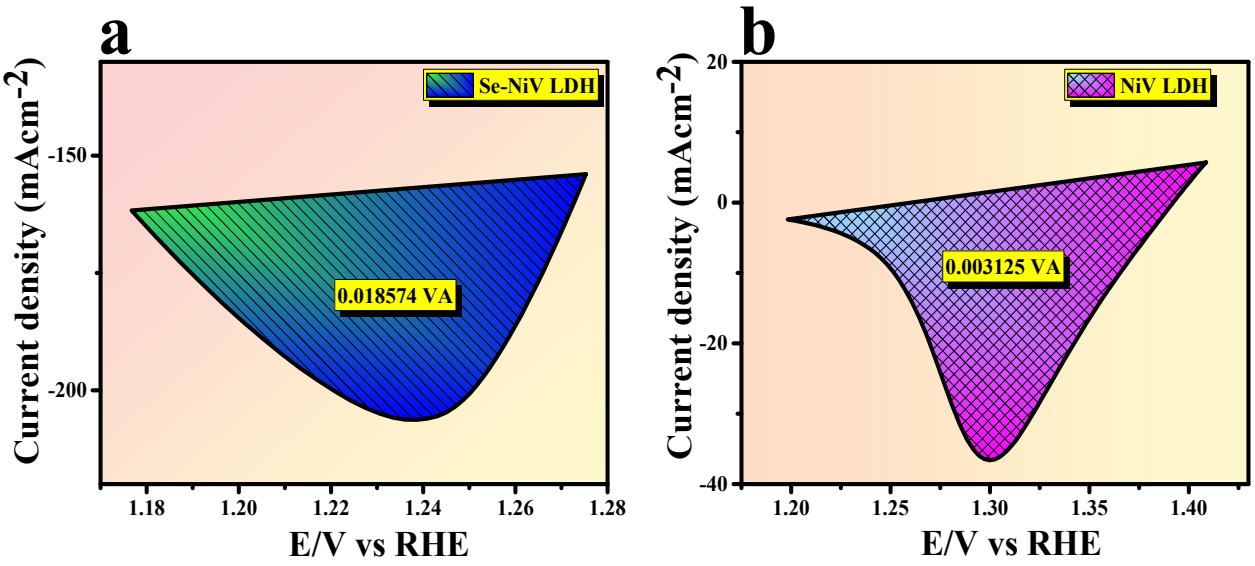

Figure S8: *(a,b) are the area of the reduction peaks for Se-NiV LDH and NiV LDH respectively.*

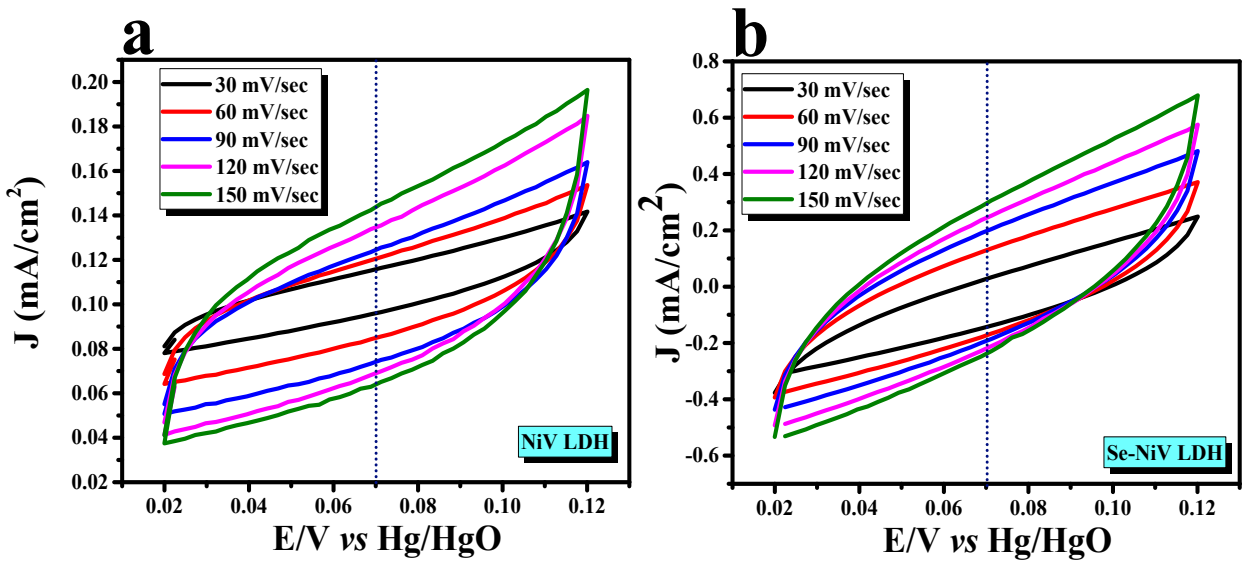

Figure S9: *(a),(b) shows the CVs recorded for NiV LDH and Se-NiV LDH in a non-faradaic region at various scan rate for the determination of ECSA from its double layer capacitance in 1M KOH solution.*

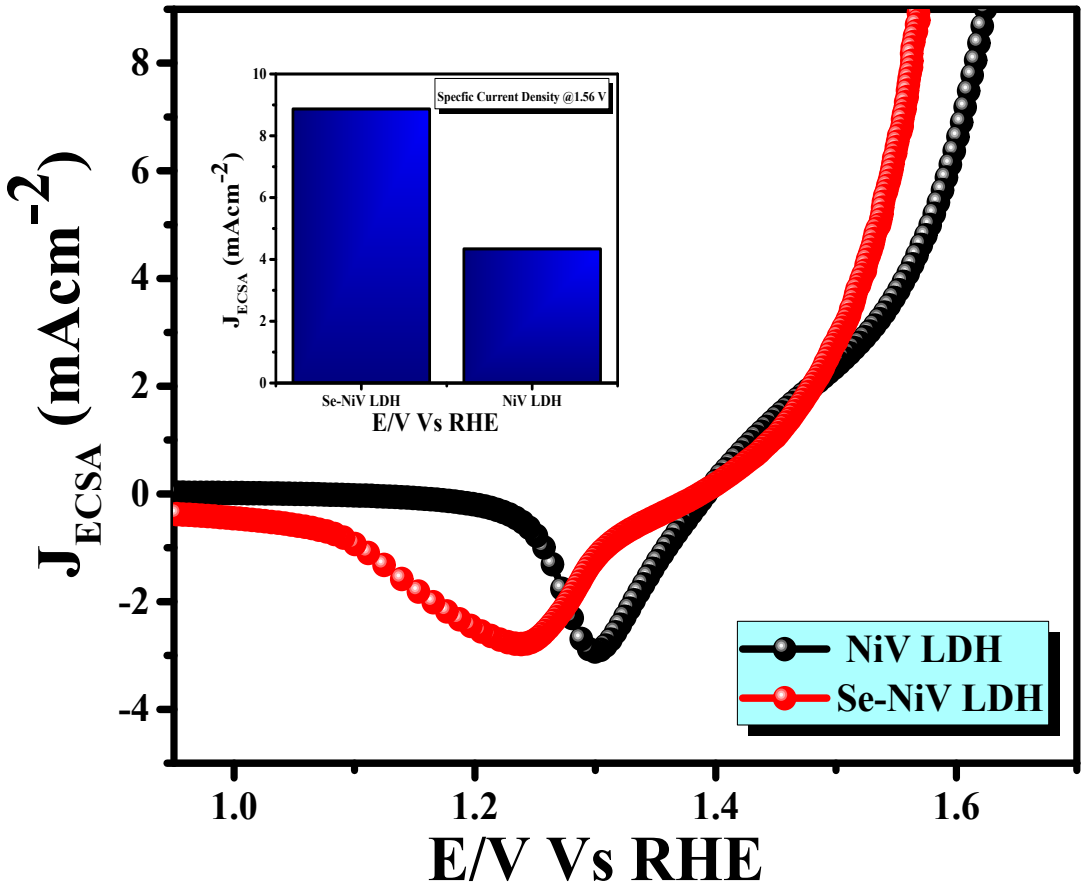

Figure S10: *ECSA normalized polarization curve for Se-NiV LDH and NiV LDH along with an inset diagram for J_{ECSA} at 1.56 V vs RHE.*

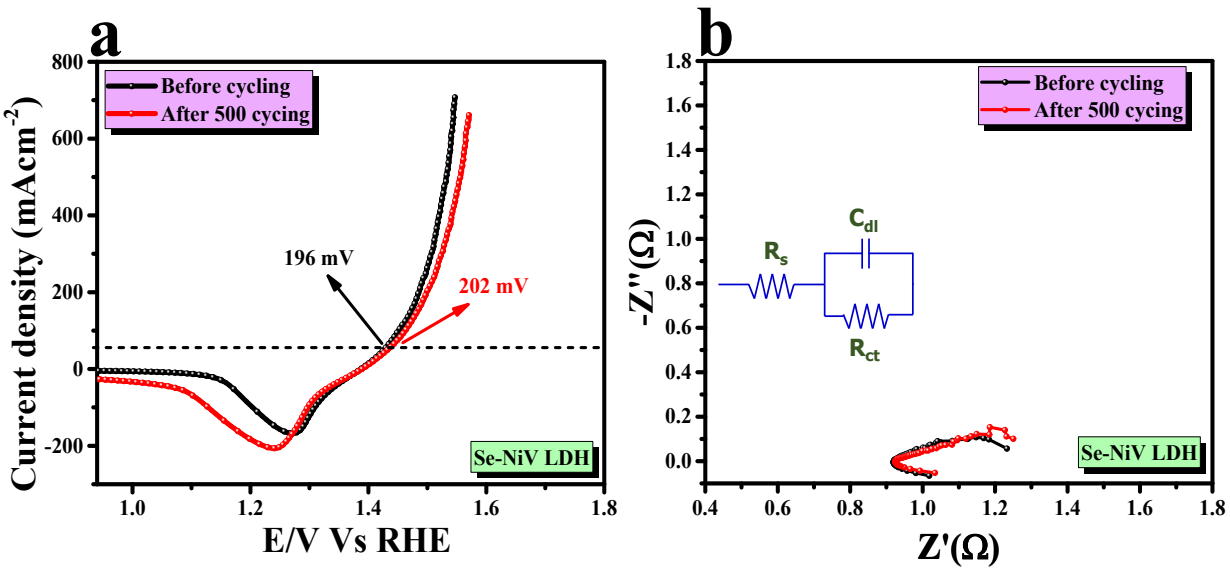

Figure S11: *(a) LSV curve of Acceleration degradation study (AD) of NiV LDH and Se-NiV LDH for OER after 500 cycles. (b) The corresponding EIS spectra in 1M KOH electrolyte.*

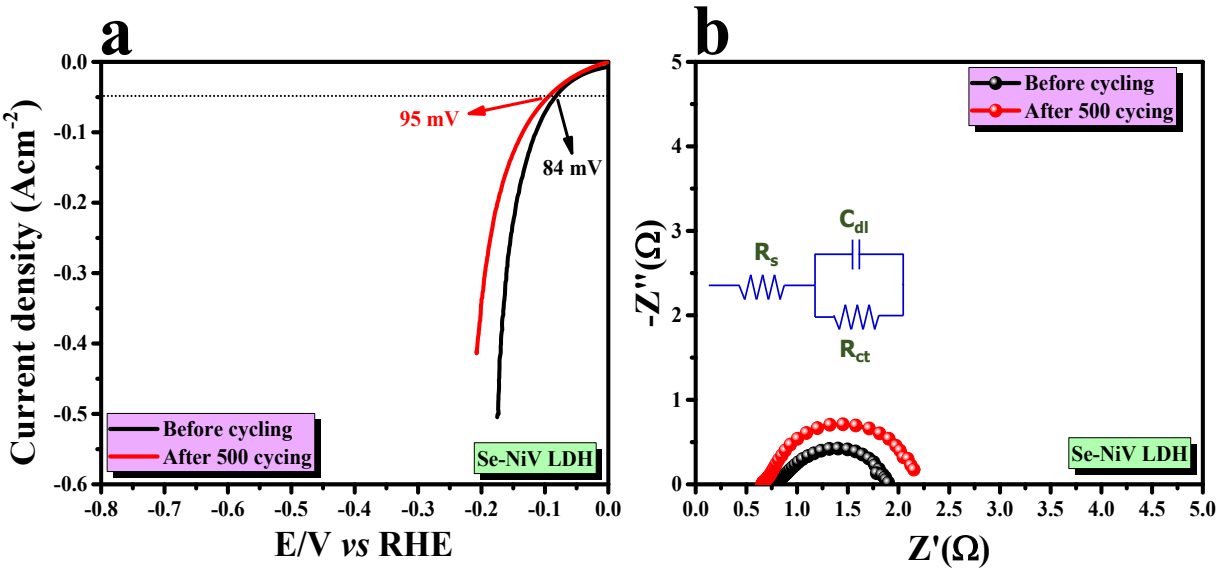

Figure S12: *(a) LSV curve of Acceleration degradation study (AD) of NiV LDH and Se-NiV LDH for HER after 500 cycles. (b) The corresponding EIS spectra in 1M KOH electrolyte.*

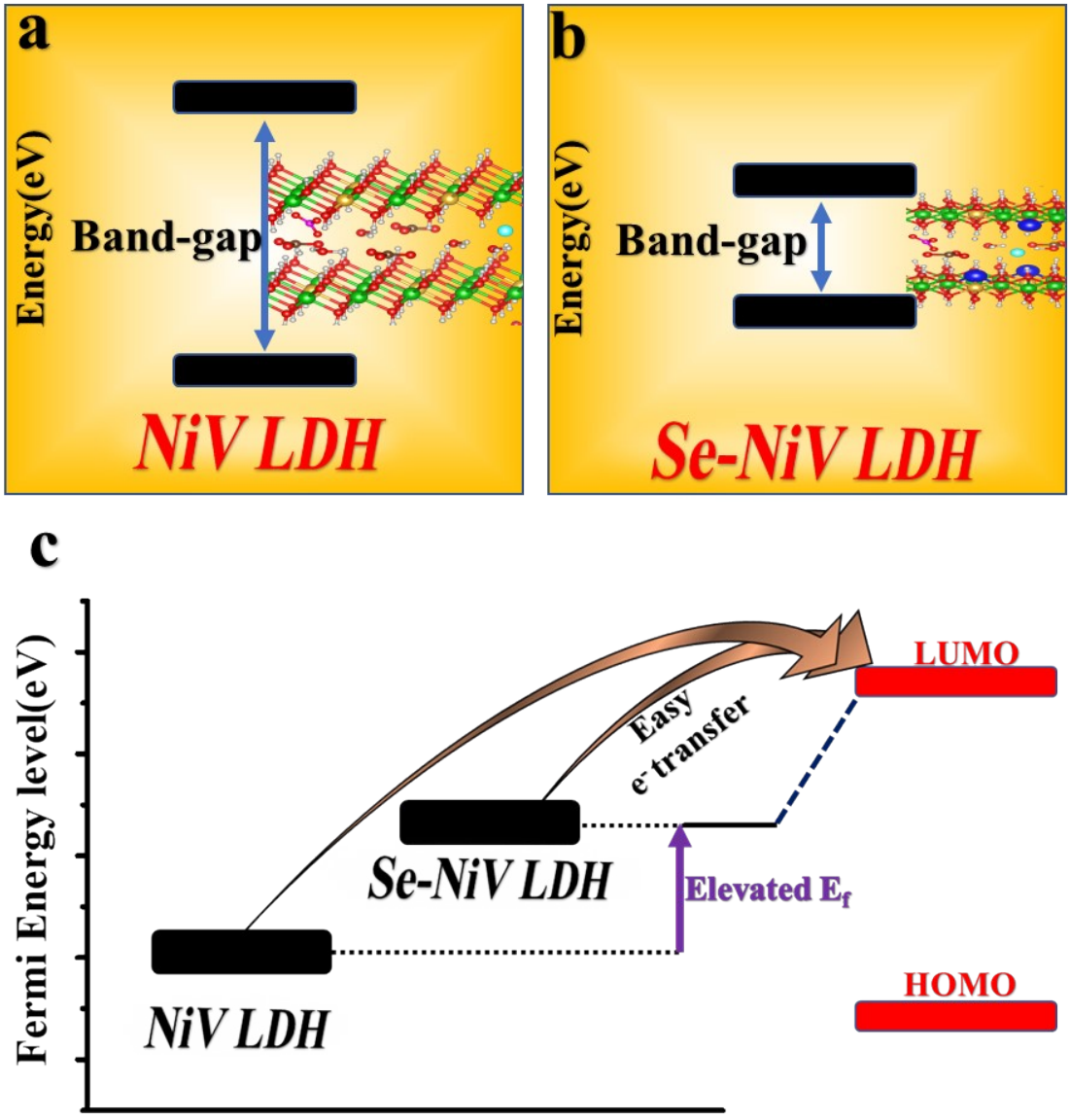

Figure S13: *(a,b) Predicted Band structures of NiV LDH and Se-NiV LDH respectively near Fermi-energy level (c) Fermi energy level comparison for NiV LDH and Se-NiV LDH.*

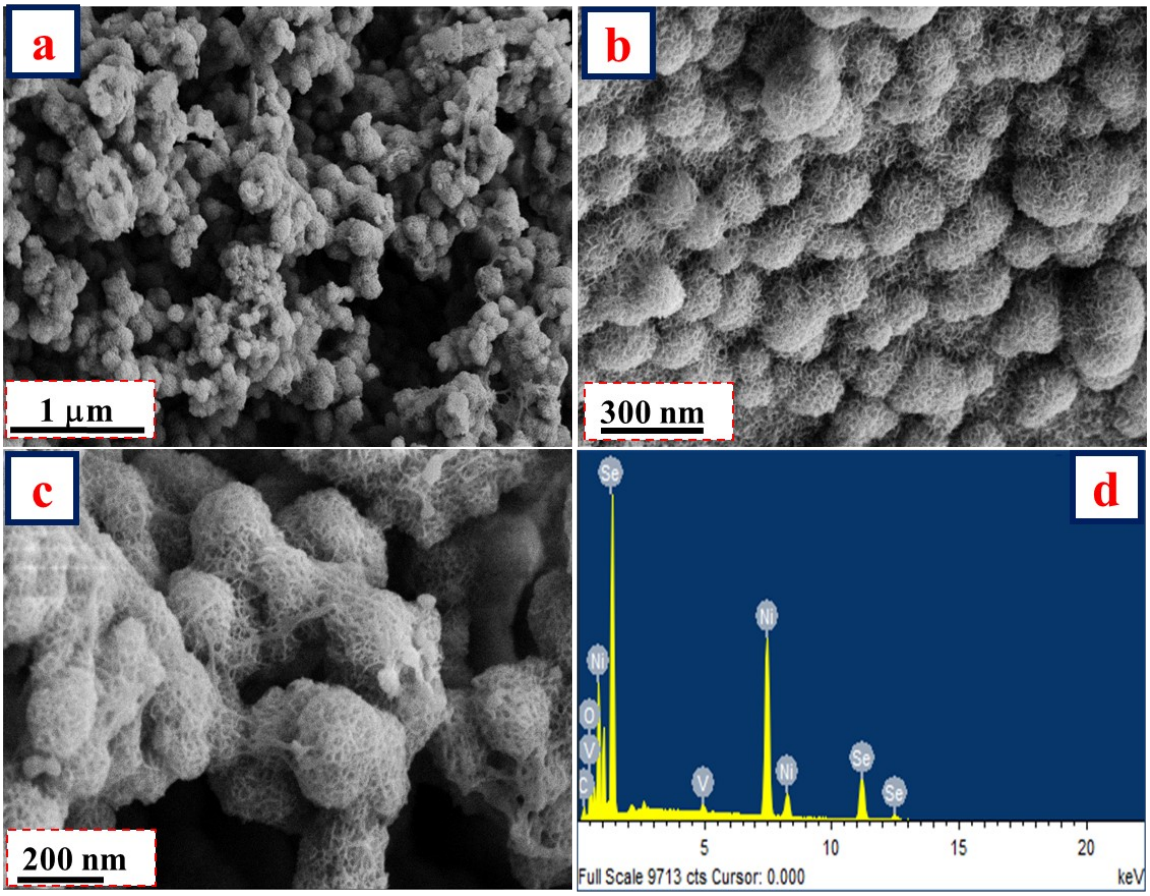

Figure S14: *(a-c) Low to high magnified FE-SEM images of post OER Se-NiV LDH. (d) EDS spectrum of post OER Se-NiV LDH.*

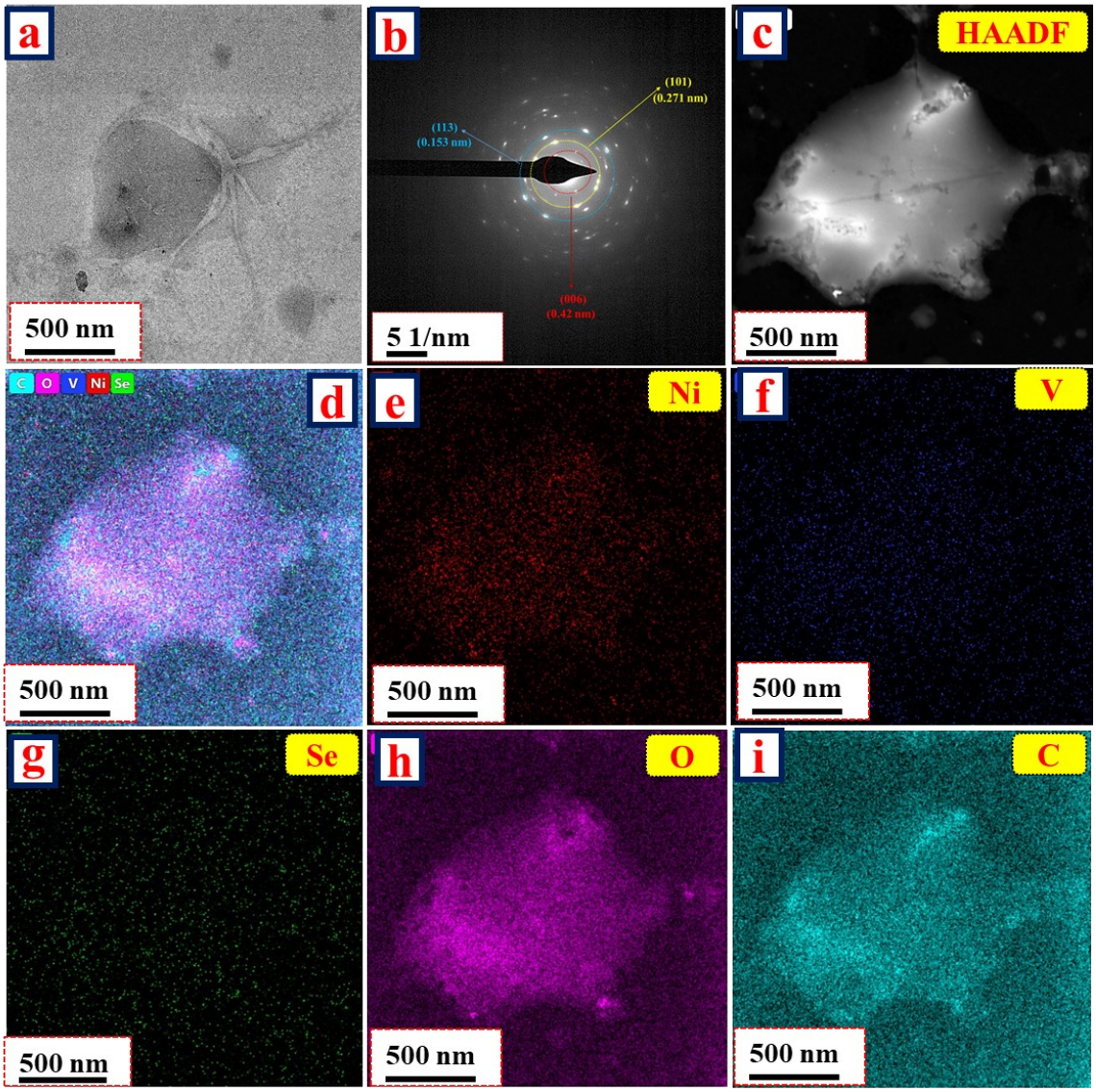

Figure S15: *(a) High magnified HRTEM images of post OER Se-NiV LDH. (b) SAED pattern of post OER Se-NiV LDH. (c) HAADF image of post OER Se-NiV LDH taken for mapping analysis. (d-i) are the corresponding characteristic colour mapping results of mix, Ni, V, Se, O, and C, respectively.*

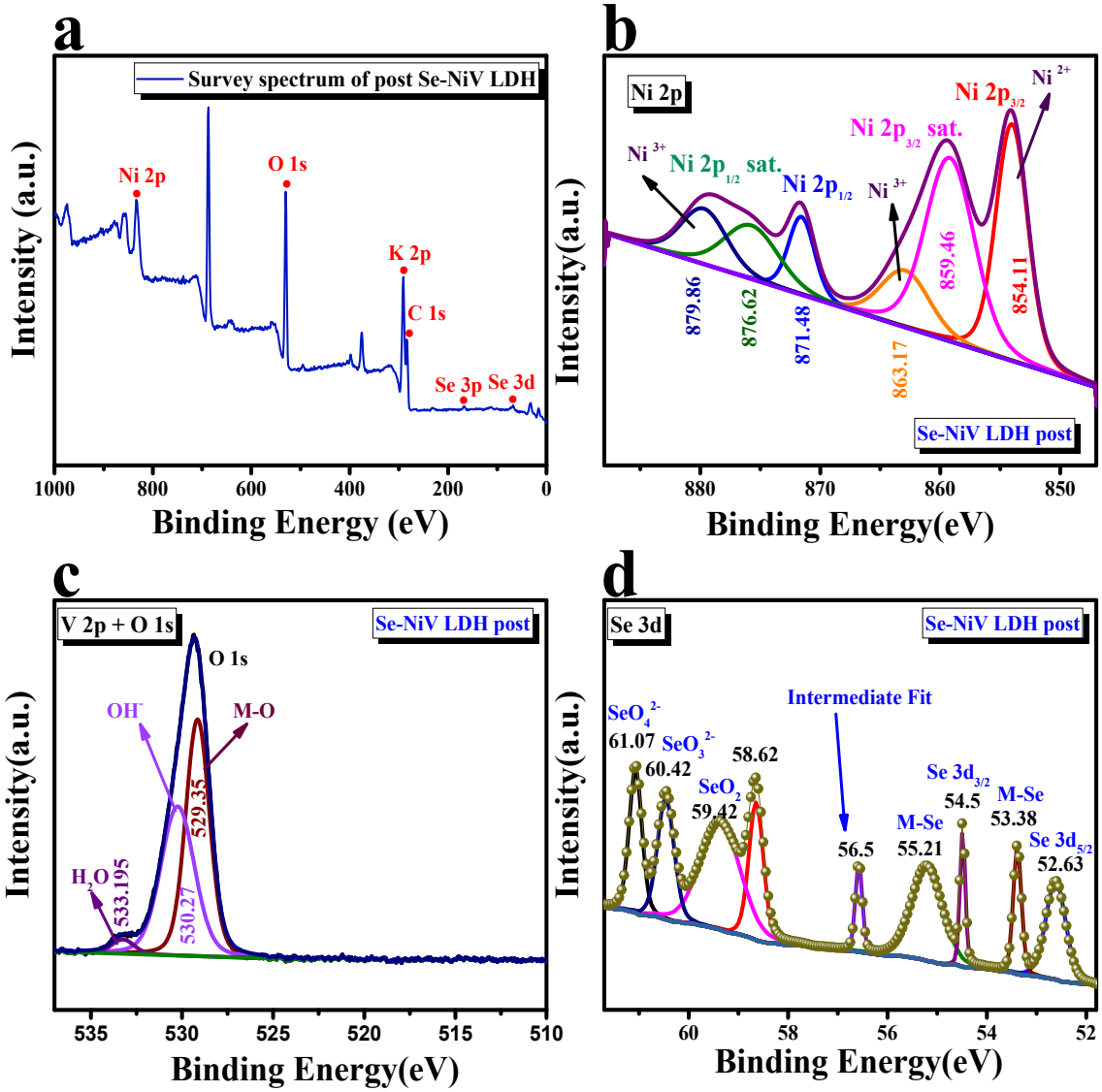

Figure S16: *(a) The deconvoluted post-XPS Survey spectra; (b) Deconvoluted post-OER XPS spectra of Ni 2p orbitals. (c) Deconvoluted post- OER XPS spectra of V 2p+O 1s orbitals, and (d) Deconvoluted post- OER XPS spectrum of Se 3d orbitals of Se-NiV LDH.*

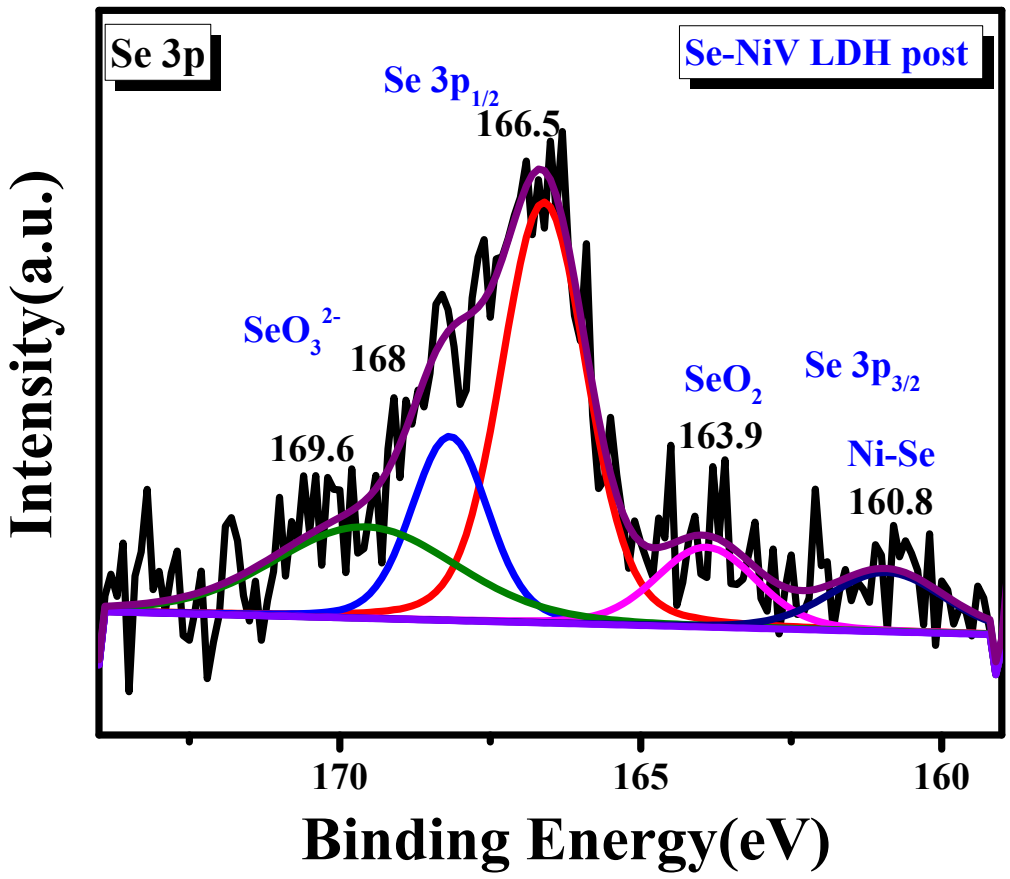

Figure S17: *(a) Deconvoluted post- OER XPS spectrum of Se 3p orbitals of Se-NiV LDH.*

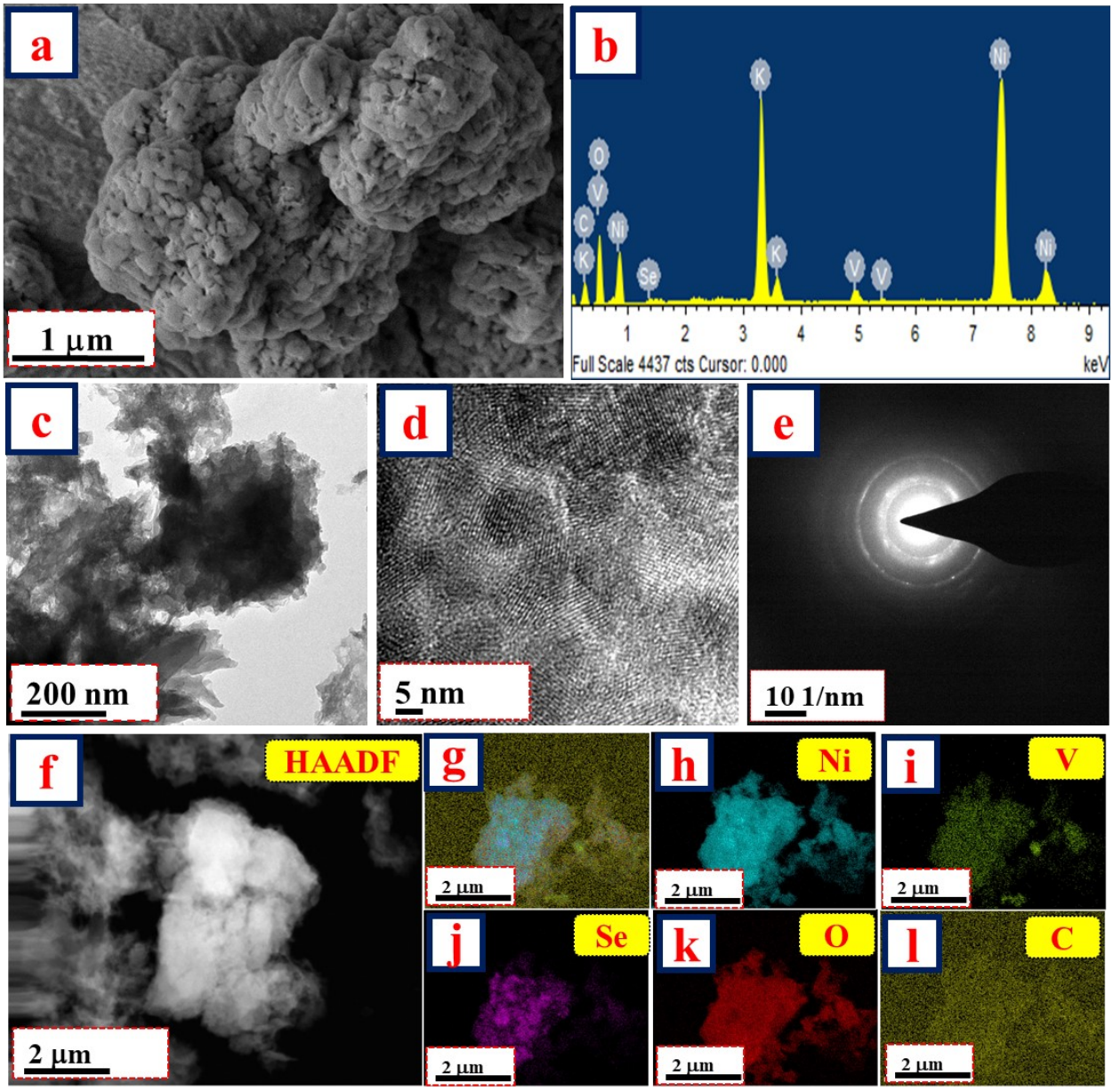

Figure S18: *(a) FE-SEM image of post HER Se-NiV LDH. (b) EDS spectrum of post HER Se-NiV LDH. (c,d) HRTEM image of post HER Se-NiV LDH. (e) SAED pattern of post HER Se-NiV LDH. (f) HAADF image of post HER Se-NiV LDH taken for mapping analysis. (g-l) are the corresponding characteristic colour mapping results of mix, Ni, V, Se, O, and C, respectively.*

Table S1: Comparison table for OER activity of Se-NiV LDH with similar type of catalyst.

Sl. No	Catalyst	Overpotential (mV)	Current density (mA/cm^2)	Reference
1	$Ni_3V_1Fe_1$ LDH	269	10	1
2	V-Ni_3Se_2	370	500	2
3	Ni_3S_2@NiV-LDH/NF	190	10	3
4	NiS/VS	240	10	4
5	NiFeS/CoS	170	50	5
6	$Ni_{0.8}Fe_{0.2}$-m/t-$Se_{0.02}$-LDH	200	10	6
7	S-NiFe LDH	259	100	7
8	S-NiFe-LDH-A	270	50	8
9	NMS	280	10	9
10	Se-NiV LDH	198	50	This work

Table S2: Comparison table for HER activity of Se-NiV LDH with similar type of catalyst.

Sl.No	Catalyst	Overpotential (mV)	Current density (mA/cm^2)	Reference
1	V-Ni_3Se_2	275	500	2
2	Ni_3S_2@NiV-LDH/NF	126	10	3
3	NiS/VS	158	10	4
4	NiFeS/CoS	150	50	5
5	NiVRu-R	48	100	10
6	NF@NiFe-LDH-1.5-4	84	100	11
7	$NiP_{1.93}Se_{0.07}$	84	10	12
8	$FeNi_2Se_4$-FeNi LDH	106	10	13
9	Se-NiV LDH	85	50	This work

SI. No	Catalyst	Potential (V)	Electrolyte	Current density (mA/cm^2)	Reference
1	V-Ni_3Se_2	1.56	1.0M KOH	10	2
2	Ni3S2@NiV-LDH/NF	1.53	1.0M KOH	10	3
3	NiS/VS	1.64	1.0M KOH	10	4
4	NiFeS/CoS	1.81	1.0M KOH	50	5
5	$FeNi_2Se_4$-FeNi LDH	1.56	1.0M KOH	10	13
6	Co_9S_8-$CoSe_2$	1.66	1.0M KOH	10	14
7	Se-NiV LDH	1.54	1.0M KOH	10	This work

Table S3: Comparison table for total water splitting activity of Se-NiV LDH with similar type of catalyst.

Reference

1 Z. Wang, W. Liu, Y. Hu, L. Xu, M. Guan, J. Qiu, Y. Huang, J. Bao and H. Li, *Inorg Chem Front*, 2019, **6**, 1890–1896.

2 D. He, L. Cao, J. Huang, Y. Feng, G. Li, D. Yang, Q. Huang and L. Feng, *ACS Sustain Chem Eng*, 2021, **9**, 12005–12016.

3 Q. Liu, J. Huang, Y. Zhao, L. Cao, K. Li, N. Zhang, D. Yang, L. Feng and L. Feng, *Nanoscale*, 2019, **11**, 8855–8863.

4 K. Bao, Y. Yan, T. Liu, T. Xu, J. Cao and J. Qi, *Inorg Chem Front*, 2020, **7**, 4924–4929.

5 J. Tang, X. Jiang, L. Tang, Y. Li, Q. Zheng, Y. Huo and D. Lin, *Dalton Transactions*, 2021, **50**, 5921–5930.

6 S. Duan, S. Chen, T. Wang, S. Li, J. Liu, J. Liang, H. Xie, J. Han, S. Jiao, R. Cao, H.-L. Wang and Q. Li, *Nanoscale*, 2019, **11**, 17376–17383.

7 H. Lei, L. Ma, Q. Wan, S. Tan, B. Yang, Z. Wang, W. Mai and H. J. Fan, *Adv Energy Mater*, 2022, **12**(48), 2202522.

8 Y.-N. Zhou, W.-L. Yu, Y.-N. Cao, J. Zhao, B. Dong, Y. Ma, F.-L. Wang, R.-Y. Fan, Y.-L. Zhou and Y.-M. Chai, *Appl Catal B*, 2021, **292**, 120150.

9 J. Du, Z. Zou, A. Yu and C. Xu, *Dalton Transactions*, 2018, **47**, 7492–7497.

10 X. Chen, J. Wan, M. Zheng, J. Wang, Q. Zhang, L. Gu, L. Zheng, X. Fu and R. Yu, *Nano Res*, 2023, **16**, 4612–4619.

11 X. Li, C. Liu, Z. Fang, L. Xu, C. Lu and W. Hou, *Small*, 2022, **18** (2), 2104354.

12 J. Zhuo, M. Cabán-Acevedo, H. Liang, L. Samad, Q. Ding, Y. Fu, M. Li and S. Jin, *ACS Catal*, 2015, **5**, 6355–6361.

13 H. Yu, Y. Xie, L. Deng, H. Huang, J. Song, D. Yu, L. Li and S. Peng, *Inorg Chem Front*, 2022, **9**, 146–154.

14 S. Chakrabartty, S. Karmakar and C. R. Raj, *ACS Appl Nano Mater*, 2020, **3**, 11326–11334.